Kinetics of Dyeing in Continuous Circulation with Direct Dyes: Tencel Case

M.J. Lis[1,*], Fabricio Maesta Bezerra[2], Xu Meng[3], Hongfei Qian[3] and A.P.S. Immich[4]

[1]*INTEXTER-UPC, Colon, 15. 08222. Terrassa, Barcelona, Spain*

[2]*Universidade Tecnológica de Paraná, Brazil*

[3]*Shaoxing University, China*

[4]*Universidade Federal de Santa Catarina, Engineering, Brazil*

Abstract: Due to the special characteristics of Tencel fibres, it is important to gather new data and information in order to improve our knowledge of their performance during dyeing. Kinetic equations are used to describe the behaviour of the heterogeneous dye-fibre system under isothermal conditions in order to determine the evolution of dye exhaustion versus dyeing time. Direct dyes are particularly suitable because they are physically absorbed and because they exhibit outstanding substantivity to cellulose. In addition, some of these dyes have a linear structure which ensures good correlation with structural differences in the fibres.

The aim of this study is to quantify the kinetic behaviour of the Tencel-C.I. Direct Blue 1 system (one of the most common dyes in dyeing studies) by using three bi-parametric empirical dyeing-rate equations and a continuous-flow dyeing cell to obtain experimental data at six different temperatures: 30, 40, 50, 60, 70 and 80ºC. In order to check the level of adjustment of the equations we record the at three exhaustion levels: 50%, 80%, and final exhaustion.

Keywords: Tencel, kinetics, direct dyes, activation energy.

1. INTRODUCTION

Cellulosic fiber, mainly cotton, is the main raw material for the textile industry. However, the difficulty of planting led to a reduction in cotton production, which resulted in increased demand for wood-based cellulose fibers. These fibers are high performance and find applications in industrial textiles, home textiles, clothing, etc. [1]. The size of cellulosic fiber market exceeded USD 17.5 billion in 2015 and an increase of more than 9.0% is estimated by the CAGR (Compound Annual Growth Rate). The global apparel market has been estimated at more than USD 1 trillion in 2015 and demand is expected to increase in the period of 2016-2024 [2].

Fibers of cellulosic origin can be divided into three main groups, such as, natural, artificial (man-made) and nanofibers. The most widely used example of man-made cellulosic fiber in the industry is viscose, but due to the non-ecological nature of its production, the valorization of Tencel fibers is increasing [3].

Tencel® fibers can be obtained by dry jetwet spinning the Lyocell®/NMMO/water by coagulating (in water or NMMO aqueous solution), washing, drying and post-treatment. This process is considered to be environmentally friendly because the solvent NMNO (N-Methylomorpholine-N-Oxide) is recovered, purified and recycled [4]. Another advantage of Tencel® spinning process is the possibility of modifying the cellulosic fibers by introducing the desired modifier into the spinning solution. Thus, fibers with superior properties such as antibacterial, luminescent, magnetic, thermochromic can be produced [3,5].

Tencel® also has high potential as technical textiles, in addition to traditional textiles, such as functional coating materials, technical fabrics, fibrous powder for plastics as a reinforcement, a special textile fiber for seat covers, etc. [6].

One of the resources to increase the value added and to extend an application of Lyocell® fibers is coloring [7]. The colorants used for Lyocell® dyeing are the same as those used for cotton dyeing [8]. However, Babar and coworkers report that Lyocell® fibers subjected to reactive dyes show better color yield when compared to cotton fibers with the same amount of colorant studied [8,9].

Environmental issues related to waste disposal, as well as high consumption of water and energy have long been taken very seriously by textile industries, especially those with dyeing stages. Therefore, a higher color intensity for the same amount of dye for lyocell fibers may lead to a more economical and ecological dyeing process [8,10]. Post-dyeing lyocell fibers with the reactive dyes, direct dyes or vat dyes is still the dominant dyeing method [7].

---

[*] Address correspondence to this author at the INTEXTER-UPC, Colon, 15. 08222. Terrassa, Barcelona, Spain; Tel: +34937398277; Fax: +34937398272; E-mail: manuel-jose.lis@upc.edu

Several wax analysis studies [11] using different alkali treatments and SEM measurements showed that Lyocell® fibres have a skin-core microstructure [4]. These two components differ in thickness and macromolecular organization, both in the radial direction. Consequently, the motion of dye molecules caused by the diffusion mechanism is expected to be different in each component, which can affect the kinetics of overall dye absorption.

Another study carried out by Ibbett and coworkers pointed out that the excellent dyeing characteristics of the Lyocell® fiber is due to its highly interconnected laminar nature of the interfibrillar pore spaces [12].

Previous studies of Carrillo and co-workers aimed at characterizing the equilibrium behaviour of Lyocell fibres with direct dyes have successfully used Chlorazol Sky Blue FF (C.I. Direct Blue 1) to determine the internal volume from Freundlich isotherms and thermodynamic parameters such as enthalpy and entropy [13]. The model proposed by Carrillo allows predicting the experimental results of a dyeing process such as the equilibrium saturation uptake of dye by the fiber and also predicting the bath exhaustion for a given concentration of dye under the experimental conditions of temperature and electrolyte concentration used [13]. Peters and Vickerstaff's and other thermodynamic models have established the physical significance of the accessible internal volume term (V). The Peters and Vickerstaff model assumes that the chemical potential for a direct dye can be expressed in terms of its activity [12]. The approximation is also made using electrolyte-solution theory that the activity of the dye corresponds to the product of the concentrations of its constituent ions [12].

The main objective of this paper is to study the kinetic behaviour of Tencel fibres with direct dyes using the known kinetic equations. The empirical models used to quantify the differences in kinetics of this dye-fibre system were chosen to include di- and tri-parametric expressions in order to evaluate the relative sensitivity to the amount of parameters included in the equations and to adapt to the different stages in the dyeing process until equilibrium is reached.

2. EXPERIMENTAL

2.1. Materials

Tencel fabric was supplied by Courtaulds Textiles, Ltd (UK). The specifications are shown in the following Table **1**:

Table 1: Specifications of Tencel Fabric Used in this Study

Density (yarns/cm)	(warp) 38 (weft) 21
Torsion	(warp) 368.8 Z (weft) 269Z
Fibres count (dtex)	1.7
Ligament	3e1b3.1
Weight (g/m^2)	325.3

Samples were washed with non-ionic detergent (Sandozine NIA, Clariant) to eliminate spin finishes and any other type of added substance that the fabric might contain. The fabric was washed at 60ºC for 60 minutes with a liquor-to-goods ratio of 12:1. Samples were rinsed several times with grade 3 water and dried at room temperature.

The electrolyte NaCl (Panreac) was used as a synthesis-grade reagent.

Chorazol Sky Blue FF (C.I. Direct Blue 1) was kindly supplied by Robama S.A. and used in the commercial form (purity 36.7 %).

2.2. Dyeing Process

The initial dye bath concentration in all experiments was 0.05 g/L and the liquor-to-goods ratio was 50:1.

The level of dye exhaustion was measured spectrophotometrically (Shimadzu UV-240) at a wavelength of 620 nm (maximum wavelength, λ_{max}) in a thermostatized continuous-flow quartz cuvette with a light path of 1 mm. The calibration curves were determined in continuous flow for each temperature and salt concentration to calculate the dye concentration that remained in the bath.

The rate flow was of 6 L/h, which equates to 0.4 cycles/minute (or 20 L/kg.min) and is very close to the mean industrial flow rates in yarn package dyeing.

2.3. Kinetic Parameters

We analyzed the kinetic behaviour of Tencel fibres to determine the evolution of the amount of direct dye absorbed at 30, 40, 50, 60, 70 and 80 ºC and with three levels of electrolyte (NaCl) concentration: 0.5, 1.0 and 1.5 g/L.

In order to avoid excessive explanation of all levels of exhaustion for all the equations, and to detect possible differences in the kinetic behaviour with the exhaustion degree in kinetic profile, the results were divided into three groups, corresponding to 50, 80 and 100 % of the final exhaustion obtained. These values were selected after consulting the study carried out by Shibushaba [14] to compare different empirical equations, in which it is demonstrated that kinetic behaviour shows different ranges of C_t/C_∞ that should be taken into account: approximately 0.5 and 0.8.

3. RESULTS AND DISCUSSION

Figures **1**, **2** and **3** show the experimental results for the evolution of C_t/C_∞ vs. the square root of time.

We obtained the values of the kinetic parameters from the experimental results (Figures **1**, **2** and **3**) and by applying non-linear regression software packages based on the Levenberg-Marquardt algorithm [15] to the following semi-empirical equations. The results are shown in Tables **2-10**:

3.1. Cegarra-Puente-Valldeperas Equation [16]

$$\frac{C_t}{C_\infty} = \left[1-\exp\left(-k*t\right)^a\right]^{1/2} \tag{1}$$

Where *k* is the apparent kinetic constant and *a* is an experimental adjustment parameter for high-exhaustion

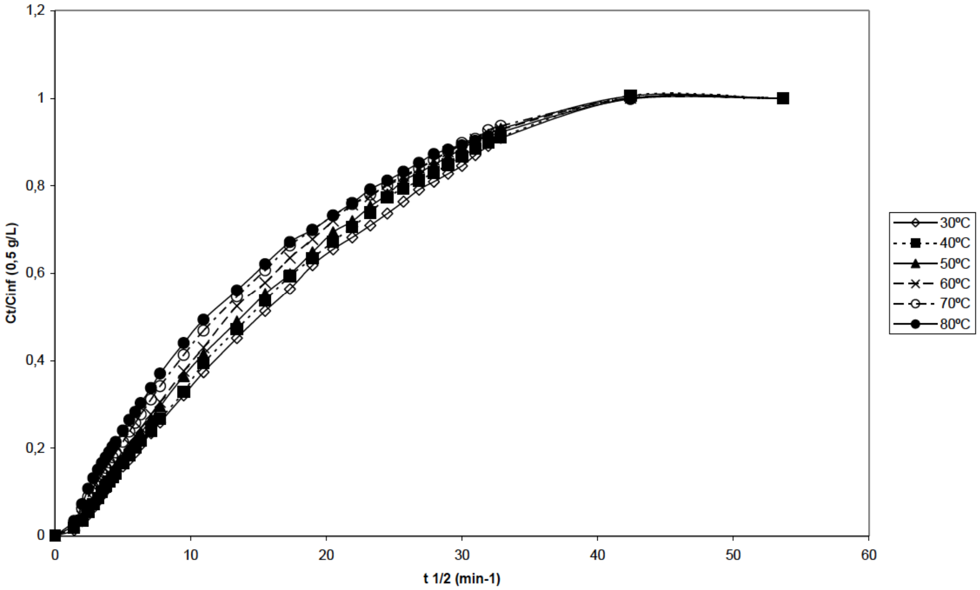

Figure 1: Evolution of C_t/C_∞ vs. square root of time for 0.5 g/L of NaCl at 30, 40, 50, 60, 70 and 80 ºC.

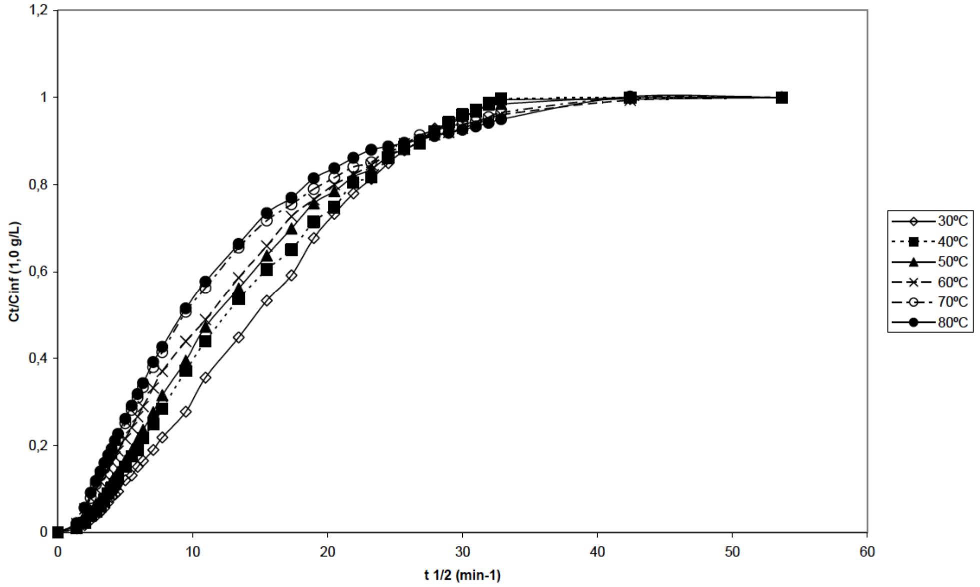

Figure 2: Evolution of C_t/C_∞ vs. square root of time for 1.0 g/L of NaCl at 30, 40, 50, 60, 70 and 80 ºC.

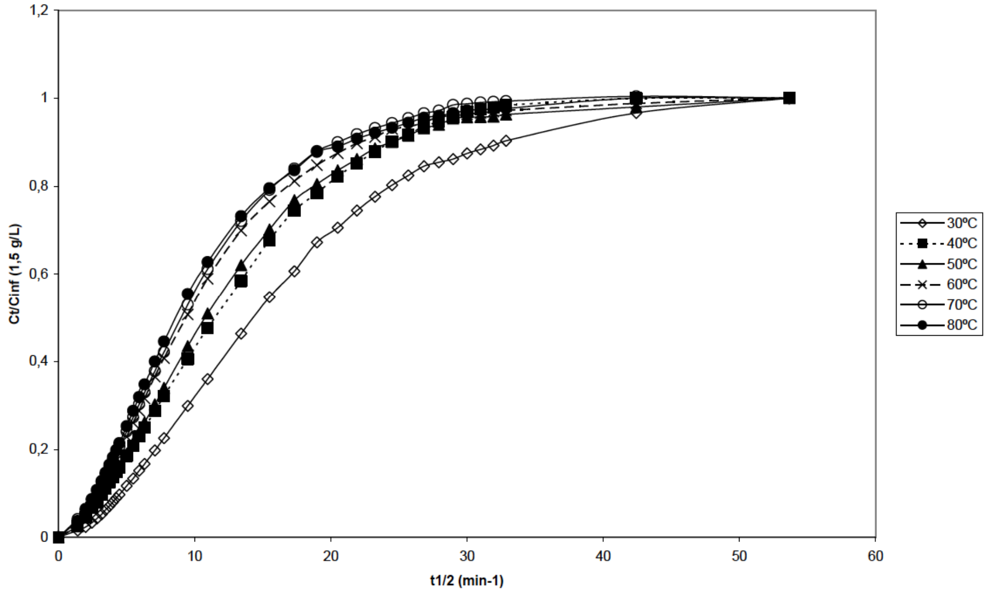

Figure 3: Evolution of C_t/C_∞ vs. square root of time for 1.5 g/L of NaCl at 30, 40, 50, 60, 70 and 80 ºC.

dyeing systems that facilitates mathematical analogies with some approximations to Fick's second law for short periods of time [17].

3.2. Chrastil's Equation [18,19,20,21]

$$\frac{C_t}{C_\infty} = \left[1 - \exp\left(-k' t\right)\right]^n \qquad (2)$$

k' is the product of the apparent kinetic constant and the absorbate concentration and *n* is an experimental constant related to the polymer resistance to dye diffusion.

3.3. Urbanik's Equation [22]

$$\frac{C_t}{C_\infty} = \left[1 - \exp\left(-kt^a\right)\right]^b \qquad (3)$$

The parameters *a* and *b* provide a better approximation to experimental results and *k* is the apparent kinetic constant.

3.4. Effect of Temperature and Electrolyte Concentration

The kinetic parameters are shown in Table **2** for 0.5 g/L of NaCl, in Table **3** for 1.0 g/L of NaCl and in Table **4** for 1.5 g/L of NaCl for the 100 % exhaustion level:

The results are shown in Table **5** for 0.5 g/L of NaCl, in Table **6** for 1.0 g/L of NaCl and in Table **7** for 1.5 g/L for the 80 % exhaustion level.

The results are shown in Table **8** for 0.5 g/L of NaCl, in Table **9** for 1.0 g/L and in Table **10** for 1.5 g/L for the first stage of the dyeing process (50 % exhaustion level).

With Eq. (1) the increase in kinetic constants between 30 and 80 ºC is sensitive to the electrolyte concentration at all three levels of exhaustion studied. The *a* parameter increases slightly with temperature by the same factor as values of *k* but with a higher maximum electrolyte concentration.

Table 2: Kinetic Parameters for the Maximum Exhaustion Level with 0.5 g/L NaCl

[NaCl] 0.5 g/L	Equation (1)		Equation (2)		Equation (3)		
T(ºC)	k (min^{-1})	a	k(min^{-1})	n	k(min^{-1})	a	b
30	2,088x10^{-3}	0,6266	1,564x10^{-3}	0,5770	1,318x10^{-3}	1,1864	0,5770
40	2,177x10^{-3}	0,6531	1,691x10^{-3}	0,5743	1,376x10^{-3}	1,2337	0,5743
50	2,268x10^{-3}	0,6811	1,774x10^{-3}	0,5582	1,403x10^{-3}	1,2635	0,5582
60	2,372x10^{-3}	0,7114	1,824x10^{-3}	0,5472	1,450x10^{-3}	1,3049	0,5473
70	2,477x10^{-3}	0,7434	1,880x10^{-3}	0,4983	1,382x10^{-3}	1,3091	0,4933
80	2,570x10^{-3}	0,7700	1,980x10^{-3}	0,5020	1,316x10^{-3}	1,3158	0,4529

Table 3: Kinetic Parameters for the Maximum Exhaustion Level with 1.0 g/L NaCl

[NaCl] 1.0 g/L	Equation (1)		Equation (2)		Equation (3)		
T(ºC)	k(min^{-1})	a	k(min^{-1})	n	k(min^{-1})	a	B
30	2,326x10^{-3}	0,7022	2,872x10^{-3}	0,8442	2,405x10^{-3}	1,1940	0,8444
40	2,507x10^{-3}	0,7529	2,832x10^{-3}	0,7088	2,514x10^{-3}	1,1263	0,7088
50	2,620x10^{-3}	0,7860	2,926x10^{-3}	0,6683	2,727x10^{-3}	1,0735	0,6683
60	2,756x10^{-3}	0,8268	2,606x10^{-3}	0,5540	2,454x10^{-3}	1,0622	0,5540
70	2,997x10^{-3}	0,8996	2,843x10^{-3}	0,5191	2,388x10^{-3}	1,1901	0,5191
80	3,090x10^{-3}	0,9236	2,925x10^{-3}	0,5084	2,854x10^{-3}	1,0193	0,5084

Table 4: Kinetic Parameters for the Maximum Exhaustion Level with 1.5 g/L NaCl

[NaCl] 1.5 g/L	Equation (1)		Equation (2)		Equation (3)		
T(ºC)	k(min^{-1})	a	k(min^{-1})	n	k(min^{-1})	a	b
30	2,283x10^{-3}	0,6555	2,171x10^{-3}	0,7110	1,828x10^{-3}	1,1878	0,7110
40	2,774x10^{-3}	0,8353	3,321x10^{-3}	0,6698	2,857x10^{-3}	1,1623	0,6698
50	2,845x10^{-3}	0,8541	3,460x10^{-3}	0,6592	3,017x10^{-3}	1,1364	0,6592
60	3,182x10^{-3}	0,9539	4,238x10^{-3}	0,6362	3,294x10^{-3}	1,2867	0,6362
70	3,360x10^{-3}	1,0068	4,717x10^{-3}	0,6554	4,567x10^{-3}	1,0765	0,6553
80	3,393x10^{-3}	1,0185	4,970x10^{-3}	0,6248	3,812x10^{-3}	1,2514	0,6248

Table 5: Kinetic Parameters for the 80% of Exhaustion and 0.5 g/L NaCl

[NaCl] 0.5 g/L	Equation (1)		Equation (2)		Equation (3)		
T(ºC)	k(min^{-1})	a	k(min^{-1})	n	k(min^{-1})	a	b
30	2,000x10^{-3}	0,6291	1,518x10^{-3}	0,5689	1,299x10^{-3}	1,1691	0,5689
40	2,137x10^{-3}	0,6412	1,697x10^{-3}	0,5750	1,373x10^{-3}	1,2359	0,5750
50	2,497x10^{-3}	0,7495	1,736x10^{-3}	0,5528	1,389x10^{-3}	1,2500	0,5528
60	2,352x10^{-3}	0,7055	1,945x10^{-3}	0,5537	1,397x10^{-3}	1,3496	0,5537
70	2,498x10^{-3}	0,7495	1,887x10^{-3}	0,5000	1,368x10^{-3}	1,3685	0,5000
80	2,630x10^{-3}	0,7887	1,800x10^{-3}	0,4956	1,341x10^{-3}	1,3419	0,4596

Table 6: Kinetic Parameters for the 80% of Exhaustion and 1.0 g/L NaCl

[NaCl] 1.0 g/L	Equation (1)		Equation (2)		Equation (3)		
T(ºC)	k(min^{-1})	a	k(min^{-1})	n	k(min^{-1})	a	b
30	2,132x10^{-3}	0,6168	2,637x10^{-3}	0,8020	1,711x10^{-3}	1,5404	0,8020
40	2,336x10^{-3}	0,7001	2,778x10^{-3}	0,7007	1,929x10^{-3}	1,4397	0,7007
50	2,512x10^{-3}	0,7534	3,060x10^{-3}	0,6827	2,548x10^{-3}	1,2010	0,6827
60	2,739x10^{-3}	0,8215	2,863x10^{-3}	0,5877	2,611x10^{-3}	1,0962	0,5776
70	3,056x10^{-3}	0,9169	3,377x10^{-3}	0,5597	3,058x10^{-3}	1,1043	0,5597
80	3,175x10^{-3}	0,9523	3,746x10^{-3}	0,5672	3,571x10^{-3}	1,0490	0,5672

Table 7: Kinetic Parameters for the 80% of Exhaustion and 1.5 g/L NaCl

[NaCl] 1.5 g/L	Equation (1)		Equation (2)		Equation (3)		
T(ºC)	k(min^{-1})	a	k(min^{-1})	n	k(min^{-1})	a	b
30	2,205x10^{-3}	0,6313	2,393x10^{-3}	0,7499	1,773x10^{-3}	1,3493	0,7499
40	2,609x10^{-3}	0,7820	3,426x10^{-3}	0,6863	2,557x10^{-3}	1,3398	0,6880
50	2,735x10^{-3}	0,8206	3,850x10^{-3}	0,6988	3,106x10^{-3}	1,2504	0,6988
60	3,117x10^{-3}	0,9349	5,001x10^{-3}	0,6919	4,024x10^{-3}	1,243	0,6919
70	3,227x10^{-3}	0,9680	5,567x10^{-3}	0,6984	4,860x10^{-3}	1,1454	0,6984
80	3,341x10^{-3}	1,0027	5,896x10^{-3}	0,6957	4,241x10^{-3}	1,3900	0,6957

Table 8: Kinetic Parameters for the 50% of Exhaustion and 0.5 g/L NaCl

[NaCl] 0.5 g/L	Equation (1)		Equation (2)		Equation (3)		
T(ºC)	k(min^{-1})	a	k(min^{-1})	n	k(min^{-1})	a	b
30	1,942x10^{-3}	0,5826	1,756x10^{-3}	0,6004	1,396x10^{-3}	1,2568	0,6004
40	2,032x10^{-3}	0,6095	1,882x10^{-3}	0,5977	1,446x10^{-3}	1,3014	0,5977
50	2,153x10^{-3}	0,6457	2,198x10^{-3}	0,6019	1,563x10^{-3}	1,4067	0,6019
60	2,278x10^{-3}	0,6835	2,393x10^{-3}	0,5982	1,574x10^{-3}	1,5471	0,5982
70	2,545x10^{-3}	0,7636	2,429x10^{-3}	0,5500	1,585x10^{-3}	1,5587	0,5506
80	2,797x10^{-3}	0,8391	2,676x10^{-3}	0,5393	1,635x10^{-3}	1,6359	0,5273

Table 9: Kinetic Parameters for the 50% of Exhaustion and 1.0 g/L NaCl

[NaCl] 1.0 g/L	Equation (1)		Equation (2)		Equation (3)		
T(ºC)	k(min^{-1})	a	k(min^{-1})	n	k(min^{-1})	a	b
30	1,745x10^{-3}	0,5234	2,490x10^{-3}	0,7793	1,663x10^{-3}	1,4972	0,7793
40	2,087x10^{-3}	0,6264	3,540x10^{-3}	0,7799	2,961x10^{-3}	1,1954	0,7799
50	2,192x10^{-3}	0,6577	4,164x10^{-3}	0,7782	3,304x10^{-3}	1,2456	0,7782
60	2,627x10^{-3}	0,7881	4,560x10^{-3}	0,6927	4,573x10^{-3}	1,3235	0,7581
70	2,985x10^{-3}	0,8953	5,629x10^{-3}	0,6978	3,871x10^{-3}	1,4541	0,6978
80	3,098x10^{-3}	0,9296	5,645x10^{-3}	0,6726	4,199x10^{-3}	1,3250	0,6726

Table 10: Kinetic Parameters for the 50% of Exhaustion and 1.5 g/L NaCl

[NaCl] 1.5 g/L	Equation (1)		Equation (2)		Equation (3)		
T(ºC)	k(min^{-1})	a	k(min^{-1})	n	k(min^{-1})	a	b
30	1,695x10^{-3}	0,5085	2,691x10^{-3}	0,7914	1,905x10^{-3}	1,4121	0,7914
40	2,330x10^{-3}	0,6990	3,522x10^{-3}	0,6878	1,895x10^{-3}	1,8585	0,6878
50	2,448x10^{-3}	0,7344	4,304x10^{-3}	0,7321	3,448x10^{-3}	1,2482	0,7321
60	2,826x10^{-3}	0,8480	6,053x10^{-3}	0,7581	4,573x10^{-3}	1,3235	0,7581
70	2,979x10^{-3}	0,8938	6,106x10^{-3}	0,7302	5,090x10^{-3}	1,1996	0,7302
80	3,125x10^{-3}	0,9376	7,336x10^{-3}	0,7742	4,731x10^{-3}	1,5506	0,7742

According to these results, the influence of temperature on the dyeing kinetics seems to be more sensitive to electrolyte concentration than to the concentration of the dye itself, at least at the levels considered here and particularly when the concentrations are low. The electrostatic effect on the surface of the fibre is greater at these levels of electrolyte concentration.

We did not detect any noticeable tendency of the *a* parameter in relation to the increase in temperature. It apparently remains constant for all of the experiments performed in this study.

The results obtained with Chrastil's equation show similar behaviour to those discussed above for Equation 1. Nevertheless, the values of the kinetic constants are more sensitive to high electrolyte concentration.

The resistance to diffusion factor *n* varies less when compared with parameter *a* of Eq. 1. The value of *n* tends to decrease with increasing temperature at every electrolyte concentration and at the three exhaustion levels studied. That corresponds to the origin of the equation that is a general solution of a sequential serie of chemical reactions. The first step, where diffusion is more sensitive to temperature and electrolyte concentration, is the most sensible to n values.

Although Equation 3 is tri-parametric, there are surprising correlations between the values of parameter *b* and factor *n* and the corresponding results for Equation 2. This is due to the mathematical nature of Urbanik's equation and the numerical approach used to calculate the different parameters, which are calculated simultaneously in both cases.

3.5. Activation Energy

According to the values of the apparent kinetic constant under different temperature conditions it is possible to calculate the apparent activation energy (E_a), assuming Arrhenius behaviour for dyeing kinetics.

$$k = k_0 \exp\left(-\frac{E_a}{RT}\right) \tag{4}$$

Results are shown in Table **11** for 0.5 g/L of NaCl, in Table **12** for 1.0 g/L of NaCl and in Table **13** for 1.5 g/L of NaCl.

As can be seen in the tables above, the sensitivity to temperature is higher in the early stages of the dyeing process than in the final stages.

Table 11: Apparent Activation Energy of Dyeing. 0.5g/L NaCl

[NaCl] 0.5 g/L	Equation (1)	Equation (2)	Equation (3)
E_a (kcal/mol)			
$C_t/C_\infty = 1$	0,8925	1,7766	-
$C_t/C_\infty = 0,8$	1,2376	2,1376	-
$C_t/C_\infty = 0,5$	1,9410	2,9819	0,6567

Table 12: Apparent Activation Energy of Dyeing. 1.0g/L NaCl

[NaCl] 1,0 g/L	Equation (1)	Equation (2)	Equation (3)
E_a (kcal/mol)			
$C_t/C_\infty = 1$	1,2188	2,6682	-
$C_t/C_\infty = 0,8$	1,7524	3,6172	3,0809
$C_t/C_\infty = 0,5$	3,1724	4,7486	3,5835

Table 13: Apparent Activation Energy of Dyeing. 1.5g/L NaCl

[NaCl] 1,5 g/L	Equation (1)	Equation (2)	Equation (3)
E_a (kcal/mol)			
$C_t/C_\infty = 1$	1,6387	3,8158	3,1760
$C_t/C_\infty = 0,8$	1,7446	3,7747	4,0182
$C_t/C_\infty = 0,5$	2,4238	4,1802	4,7821

The values of the apparent activation energy are lower at low electrolyte concentration. In the case of Equation 3, there are several conditions under which it is not possible to calculate the activation energy, particularly at maximum exhaustion levels.

The results suggest that, unlike other cellulosic fibres, which have been studied in depth, Tencel shows a high swelling effect. This is relevant to dye diffusion when there is strong repulsion caused by the anion-charged fibre surface, due to the use of low electrolyte concentrations. This implies that the effect of temperature on dye-fibre interactions is negligible in comparison with the effect of swelling phenomena.

Differences on the swelling behaviour could be attributed to the existence of different order structures depending on the radius of the fiber. At different levels of exhaustion, fiber shows different resistance to diffusion. That fact has been studied [17] but the diffusional approach will be the objective of other publication.

4. CONCLUSIONS

In this study we used C.I. Direct Blue as a tracer to investigate the kinetic behaviour of Tencel fibre in the 30-80 ºC temperature range and the influence of a neutral electrolyte at low concentrations. We compared three different, empirical kinetic equations used to quantify the isothermal dyeing process. No significant differences were observed in the values obtained from the three equations for characterizing the dyeing process of Tencel fibres.

The equations used show that the process is most sensitive to temperature changes in the early stages and that sensitivity increases with electrolyte concentration.

Given the strong mathematical dependence between the parameters of bi- and tri-parametric models, it is necessary to use diffusion coefficients to establish more reliable comparisons of the dyeing process under the experimental conditions used in this study.

REFERENCES

[1] Market Research Report. Cellulose Fiber Market Size and Share. Industry Report 2018-2015. Gran View Research. San Francisco. 2016, 75p.

[2] Kiran Pulidindi, Soumalya Chakraborty. Cellulose Fiber Market Trends, Industry Size Report – 2016-2024. Global market Insights. Delaware. 2017, 104p.

[3] Małgorzata Skwierczyńskaa, Marcin Runowskia, Piotr Kulpińskib, Stefan Lisa,. Modification of cellulose fibers with inorganic luminescent nanoparticles based on lanthanide(III) ions. Carbohydrate Polymers 206 (2019) 742–748. https://doi.org/10.1016/j.carbpol.2018.11.058

[4] Erdman, A., Kulpinski, P., Grzyb, T., & Lis, S. (2015). Preparation of multicolor luminescent cellulose fibers containing lanthanide doped inorganic nanomaterials. Journal of Luminescence, 169, 520–527. https://doi.org/10.1016/j.jlumin.2015.02.049

[5] Kulpinski, P., Erdman, A., Grzyb, T., & Lis, S. (2016). Luminescent cellulose fibers modified with cerium fluoride doped with terbium particles. Polymer Composites, 37, 153–160. https://doi.org/10.1002/pc.23166

[6] Wang, S., Lu, A., & Zhang, L. (2016). Recent advances in regenerated cellulose materials. Progress in Polymer Science, 53, 169–206. https://doi.org/10.1016/j.progpolymsci.2015.07.003

[7] Zhang, Liping; Sun, Weize; Xu, Dan; Li, Min; Agbo, Christiana; Fu, Shaohai. Dope dyeing of lyocell fiber with NMMO-based carbon black dispersion. Carbohydrate Polymers 174 (2017) 32–38. https://doi.org/10.1016/j.carbpol.2017.06.020

[8] Babar, Aijaz Ahmed; Peerzada, Mazhar Hussain; Jhatial, Abdul Khalique; Bughio, Noor-ul-ain. Pad ultrasonic batch dyeing of causticized lyocell fabric with reactive dyes. Ultrasonics Sonochemistry 34 (2017) 993–999. https://doi.org/10.1016/j.ultsonch.2016.07.018

[9] Shahid, M.; Hossain, M.; Hossain, D.; Ali, A. Effect of different dyeing parameters on color strength & fastness properties of cotton-elastane (CE) and lyocellelastane (LE) knit fabric, Int. J. Textile Sci. 5 (2016) 1–7. https://doi.org/10.5923/j.textile.20160501.0

[10] Taylor, J. Controlling fibrillation – experiences of the dyeing and finishing of lyocell fibres, Color. Technol. 131 (2015) 424–433. https://doi.org/10.1111/cote.12184

[11] Shurz. Was is neu an den neuen fasern der gattung Lyocell? Lenzinger Berichte (1994*)* 9, p. 38.

[12] R.N. Ibbett, D.A.S. Phillips, S. Kaenthong. Evaluation of a dye isotherm method for characterisation of the wet-state structure and properties of lyocell fibre. Dyes and Pigments 71 (2006) 168e177. https://doi.org/10.1016/j.dyepig.2005.06.010

[13] Carrillo, F., Lis, M.J, Valldeperas, J. Sorption Isotherms and behaviour of direct dyes on lyocell fibres. Dyes and Pigments. (2002); 53: pp. 129-136. https://doi.org/10.1016/S0143-7208(02)00007-4

[14] Shibushawa, T. The mathematical expression of rate constants in empirical rate of dyeing equations in disperse dyeing. J.S.D.C. (1988); 104: p. 28. https://doi.org/10.1111/j.1478-4408.1988.tb01132.x

[15] Data Fit 8.1. Oakdale Engineering Manual.

[16] Cegarra, J., Puente, P., Valldeperas, J. Fundamentos científicos y aplicados de la tintura de las materias textiles. Cátedra de Tintorería. UPB. (1981); p. 128.

[17] Lis Arias, Manuel J. Kinetic behaviour of Tencel fibres with Direct Dyes. PhD Thesis. UPC. 2002.

[18] Chrastil, J., Reinhardt, R.M., Blanchard, E.J. Influence of mercerization and crosslinking of cotton fabrics on dyeing kinetics of direct dyes from finite baths. Textile Research Journal. (1990); August: pp. 441-446. https://doi.org/10.1177/004051759006000802

[19] Chrastil, J. Adsorption of Direct Dyes on Cotton: Kinetics of dyeing from finite baths. Textile Research Journal. (1990); July: pp. 413-416. https://doi.org/10.1177/004051759006000706

[20] Chrastil. J. Enzymic product formation curves with the normal or diffusion limited reaction mechanism and in the presence of substrate receptors. Int. J. Biochem. (1988); 20:7: p. 685. https://doi.org/10.1016/0020-711X(88)90163-2

[21] Chrastil, J. Determination of the first order consecutive reaction rate constants from final product. Comput. Chem. (1988); 12:4: p. 289. https://doi.org/10.1016/0097-8485(88)80002-0

[22] Urbanik, A. A generalized form of the Cegarra-Puente equation. Relationships of Empirical Dyeing Rate equations to Diffusion parameters. Textilveredlung. (1978); 13:7: pp. 278-279.

Received on 06-04-2019 Accepted on 25-06-2019 Published on 16-07-2019

DOI: https://doi.org/10.31437/2415-5489.2019.05.10